

Falling plumes in bacterial bioconvection

By AISLING M. METCALFE AND T. J. PEDLEY

Department of Applied Mathematics and Theoretical Physics, University of Cambridge,
Silver Street, Cambridge CB3 9EW

(Received 26 September 2000 and in revised form 4 May 2001)

Experiments by Kessler on bioconvection in laboratory suspensions of bacteria (*Bacillus subtilis*), contained in a deep chamber, reveal the development of a thin upper boundary layer of cell-rich fluid which becomes unstable, leading to the formation of falling plumes. We use the continuum description of such a suspension developed by Hillesdon *et al.* (1995) as the basis for a theoretical model of the boundary layer and an axisymmetric plume. If the boundary layer has dimensionless thickness $\lambda \ll 1$, the plume has width $\lambda^{1/2}$. A similarity solution is found for the plume in which the cell flux and volume flux can be matched to those in the boundary layer and in the bulk of the suspension outside both regions. The corresponding model for a two-dimensional plume fails to give a self-consistent solution.

1. Introduction

Bioconvection is the spontaneous formation of patterns in suspensions of swimming micro-organisms. Organisms exhibiting bioconvection have two things in common: they are denser than water and they swim upwards, on average, in still water. Up-swimming causes the micro-organisms to accumulate in the upper regions of the fluid, but because they are denser than water this distribution is unstable and an overturning instability develops, leading to the formation of patterns. The process is similar to thermal convection in a fluid heated from below, hence the term bioconvection, first used by Platt (1961).

We are concerned with bioconvection in a suspension of the oxytactic bacterium *Bacillus subtilis*, which consumes oxygen and swims up oxygen gradients. In an initially well-mixed suspension, open to the air at the upper free surface, oxygen is replenished by diffusion from that surface, so an oxygen gradient develops up which the bacteria swim. There are two slightly different cases: a ‘shallow’ and a ‘deep’ chamber. In a shallow chamber the oxygen concentration throughout the chamber is high enough to allow all the bacteria to swim actively. If the chamber is deep, the oxygen concentration below a certain depth falls below that required for the bacteria to be active and an inactive zone, in which the bacteria do not swim, forms at the bottom of the chamber. Experiments in a shallow chamber, such as a petri dish, show the formation of complex labyrinthine patterns. Experiments in a tilted chamber show that no patterns form in very shallow regions, but as the depth increases hexagonal bioconvection patterns are seen and these in turn give way to the labyrinthine patterns as the depth increases further. Previous mathematical models (Hillesdon, Pedley & Kessler 1995; Hillesdon & Pedley 1996; Metcalfe & Pedley 1998) have investigated such phenomena. In this paper we consider a deep chamber.

Figure 1 shows a series of photographs, taken from the side, of bioconvection in a suspension of *B. subtilis* contained in a deep chamber made from two microscope

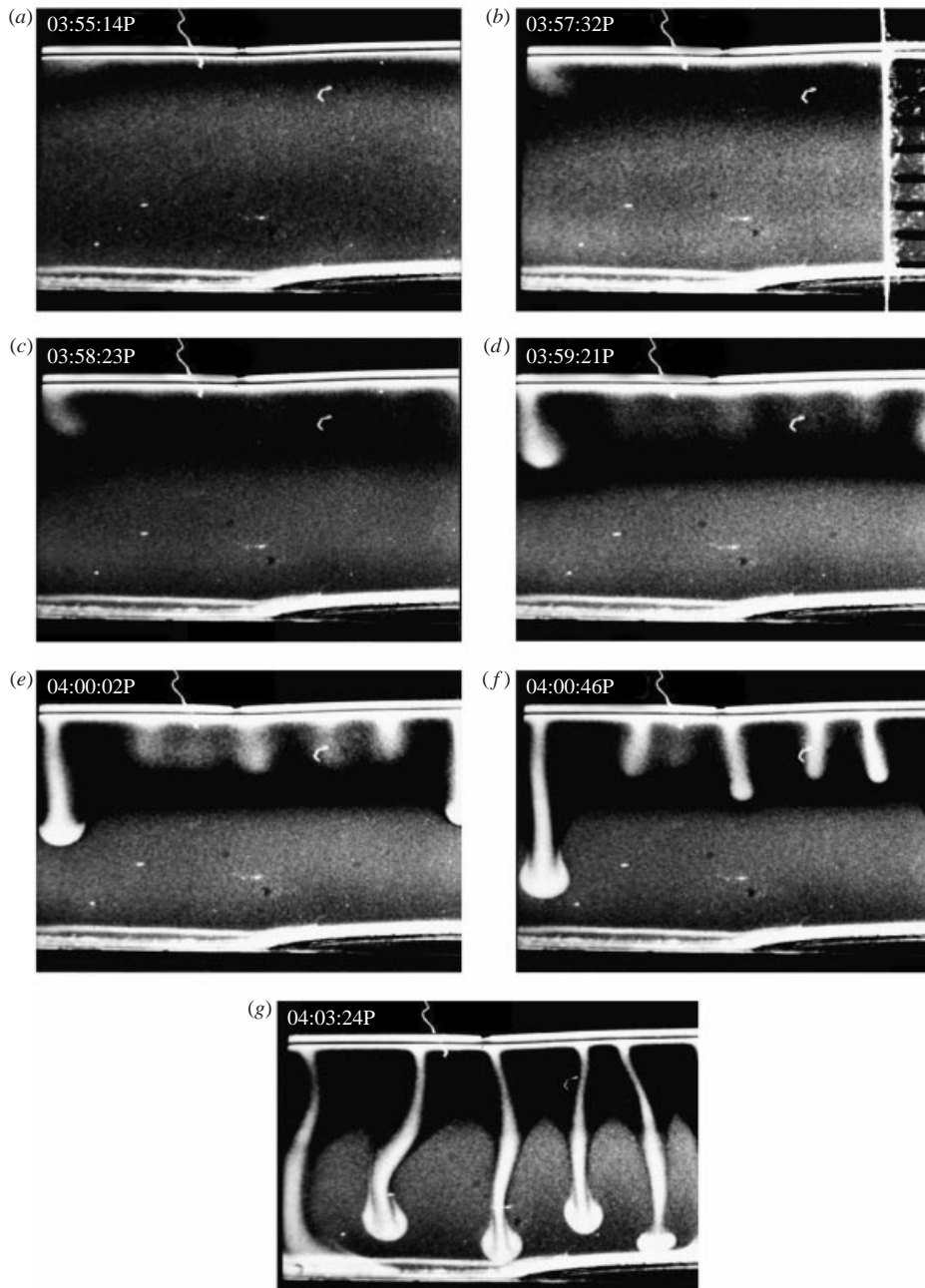


FIGURE 1. A time sequence of photographs, taken from the side, of a deep chamber (depth approximately 7–8 mm) containing a suspension of *Bacillus subtilis*. Near the surface, where significant gradients of oxygen exist, the cells swim upwards. A convective instability forms when the vertical density gradient becomes sufficiently large. Cell-rich plumes descend from the surface carrying oxygen which resuscitates the inactive cells in the lower region of the chamber. Note that the successive times are shown at the upper left of each frame. Photograph reproduced from Hillesdon *et al.* (1995).

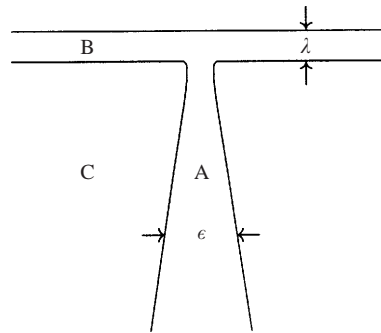


FIGURE 2. The three different regions in the plume calculation: plume (A) of width ϵ , boundary layer (B) of thickness λ , outer region (C).

slides placed vertically and held 1 mm apart (Kessler *et al.* 1994). The bottom and edges of the chamber are sealed but the upper surface is open to the atmosphere. The light regions contain a high concentration of bacteria and in figures 1(a)–1(c) we can see the development of a thin, cell-rich upper boundary layer as the bacteria swim up the oxygen gradient towards the surface. The concentration of bacteria in the region immediately below the upper layer is therefore reduced. The lower part of the chamber is too far from the surface for significant amounts of oxygen to reach it by diffusion and once the cells in this region have consumed the dissolved oxygen they become inactive. The cell concentration in this lower region remains almost constant, as can be seen by the grey layer at the bottom of figures 1(a)–1(e). In figures 1(d)–1(f) we see the formation of falling plumes of dense, cell-rich fluid descending from the upper layer as it becomes unstable. The descending plumes carry oxygen from the surface and in figure 1(g) some of the inactive cells in the lower region have been resuscitated by the oxygen carried by the descending plumes.

We will model the quasi-steady situation in which an upper boundary layer containing a high concentration of bacteria feeds a falling plume of cell-rich fluid. We consider the suspension as being divided into three separate regions, as shown in figure 2: a cell-rich upper boundary layer of known thickness λ (region B), a falling plume of unknown width ϵ which also contains a high concentration of bacteria (region A) and the fluid outside the plume (region C), which has to circulate in order to conserve mass. We will consider the problem both in three dimensions, where we will assume that the plume is axisymmetric, and in two dimensions. The results will therefore not be directly applicable to the experiments of figure 1, since the configuration there is neither axisymmetric nor two-dimensional.

The problem is only quasi-steady because the oxygen concentration is effectively zero in the lower part of the chamber so that once the bacteria in the plume reach this lower region they are unable to swim and they remain there rather than swimming back into the upper boundary layer. Our analysis covers only the upper part of the chamber in which the oxygen concentration is above zero and ignores the mixing and (partial) resuscitation that take place in the lower zone. A numerical solution would probably be required to study the full depth of the fluid.

In the case of thermal convection, similarity solutions can be obtained for a plume of warm fluid rising from a point or a line source of heat (Yih 1951, 1952) and this prompts us to seek similarity solutions for the falling plumes of cell-rich fluid such as those seen in the experiment of figure 1. As with thermal plumes from a source of finite size, the similarity solution is expected to be valid only at distances which are

large compared with the size of the source. The problem of bioconvection is more complex than the thermal convection problem since it contains two diffusing and interacting species. The problem is not one of double-diffusive convection, however, because only one of the diffusing species, the cells, contributes to the density, but a further complication is introduced by the interaction of the cells and the oxygen.

Two-dimensional convection in the limit of infinite Prandtl and Rayleigh number (fast, viscous flow) has been studied for the case of a heated strip in an infinite horizontal plane (Roberts 1977). In this limit, the heat from the heated boundaries can only penetrate thin boundary layers and thermal plumes in which the motion is driven by buoyancy forces and the fluid velocity is approximately constant across the plume. Roberts (1977) solved the heat equation in the thin layer and plume by using the stream function as a transverse coordinate and found an asymptotically valid expression for the dimensionless heat flux as the Rayleigh number tends to infinity.

It is possible that, in some bacterial experiments, chemotaxis and oxygen consumption are important only in setting up the basic state and that once this is set up the resulting plumes are entirely buoyancy driven and the cells are merely advected. In this case the plume problem would reduce essentially to that of Roberts (1977), except that the velocity would vary across the plume, or Yih (1951, 1952). However, we are investigating plumes where chemotaxis and oxygen consumption are important in the plume itself.

For gyrotactic algae, Ghorai & Hill (1999) found a model for a steady plume which is independent of the vertical coordinate. In that model, cell diffusion out of the plume is balanced by gyrotactic focusing into the plume. It is not possible to obtain a similar Z -independent solution using our model for bacterial chemotaxis since in the absence of a gyrotactic term there is nothing to balance the diffusion of cells out of the plume. Chemotaxis causes cells to swim out of the plume because the high concentration of cells in the plume leads to a lower concentration of oxygen there than in the surrounding fluid.

We first describe the axisymmetric case: in §3 we describe the solution in the upper boundary layer and in §4 we consider the falling plume and find a similarity solution for this region, analagous to that for a standard thermal plume (Yih 1951, 1952) in which the cell flux is constant. We then find a solution for the flow in the outer region, assuming that the Reynolds number is small (§5), and finally match the solutions in all three regions (§6). We find that the solutions in the different regions are consistent only if the width of the plume, ϵ , is given by $\lambda^{1/2}$; we are also able to determine the value of the cell flux. The model for the two-dimensional case is similar. We find a solution in the upper boundary layer (§7.1) and for the flow in the outer region (§7.3) but the partial differential equations governing the plume itself appear not to have a similarity solution (§7.2) and a fully numerical solution is beyond the scope of this study.

2. Governing equations

The problem is described by an equation for concentration of cells (\tilde{N}) and an equation for oxygen concentration (\tilde{C}) together with the Navier–Stokes equations (using the Boussinesq approximation) and the continuity equation. This formulation and the steady-state solution is that of Hillesdon *et al.* (1995). The dimensional equation for cell conservation is

$$\frac{\partial \tilde{N}}{\partial T} = -\nabla \cdot (\tilde{N} \tilde{U} + \tilde{N} \mathbf{V} - \mathbf{D}_N \cdot \nabla \tilde{N}), \quad (2.1a)$$

in which the cell-flux vector contains a term for advection of cells with the bulk fluid velocity $\tilde{\mathbf{U}}$ and two terms describing cell swimming. The random aspects of cell swimming are modelled by a diffusive term, where \mathbf{D}_N is the cell diffusivity, and the directional part of cell swimming is modelled by a superimposed average swimming velocity, \mathbf{V} (Keller & Segel 1971*a, b*).

The equation for oxygen conservation is

$$\frac{\partial \tilde{C}}{\partial T} = -\nabla \cdot (\tilde{C} \tilde{\mathbf{U}} - D_C \nabla \tilde{C}) - K \tilde{N}. \quad (2.1b)$$

The oxygen flux vector contains terms for advection and diffusion of oxygen, where D_C is the oxygen diffusivity. The term $-K \tilde{N}$ describes the consumption of oxygen by the bacteria where K is proportional to the rate of oxygen consumption per cell.

The governing equations contain no terms for bacterial reproduction and death or cell sedimentation since these effects are negligible on the short timescales associated with bioconvection (Hillesdon 1994). We also ignore gyrotaxis, the orientation of cells by viscous forces in a shear flow, although this has been found to be important in bioconvection of algae such as *Chlamydomonas nivalis* (Kessler 1985; Hill, Pedley & Kessler 1989; Pedley & Kessler 1990; Bees & Hill 1998); however, there is currently no quantitative model for gyrotaxis among chemotactic organisms (see Bearon & Pedley 2000 for a first approach to such a model).

The bacteria can be thought of as requiring a minimum concentration of oxygen, C_{min} , in order to be active. This is taken into account by non-dimensionalizing the oxygen concentration as

$$\theta = \frac{\tilde{C} - C_{min}}{C_0 - C_{min}},$$

where C_0 is the initial and free-surface oxygen concentration. The cell diffusion is modelled as an isotropic tensor, $\mathbf{D}_N = D_{N0} H(\theta) \mathbf{I}$ where $H(\theta)$ is the step function, the directional cell swimming as proportional to the gradient of θ , $\mathbf{V} = b V_s H(\theta) \nabla \theta$, and the oxygen consumption as $K = K_0 H(\theta)$. $b V_s$, D_{N0} and K_0 are taken to be given constants; b has dimensions of length so that V_s has dimensions of velocity.

The other variables are non-dimensionalized as:

$$N = \frac{\tilde{N}}{N_0}, \quad Z = \frac{\tilde{Z}}{h}, \quad t = \frac{D_{N0}}{h^2} T, \quad \mathbf{U} = \frac{h}{D_{N0}} \tilde{\mathbf{U}}, \quad (2.2)$$

where h is the depth of the chamber and N_0 is the initial cell concentration. The vertical coordinate Z is measured downwards so that $Z = 0$ is the free surface at the top of the chamber and $Z = 1$ is the bottom of the chamber. The non-dimensionalized equations are

$$\frac{\partial N}{\partial t} = \nabla \cdot [H(\theta) \nabla N - \mathbf{U} N - H(\theta) \gamma N \nabla \theta], \quad (2.3a)$$

$$\frac{\partial \theta}{\partial t} = \nabla \cdot (\delta \nabla \theta - \mathbf{U} \theta) - H(\theta) \delta \beta N, \quad (2.3b)$$

$$\nabla \cdot \mathbf{U} = 0, \quad (2.3c)$$

$$Sc^{-1} \left[\frac{\partial \mathbf{U}}{\partial t} + (\mathbf{U} \cdot \nabla) \mathbf{U} \right] = -\nabla P_e + \nabla^2 \mathbf{U} + \Gamma N \hat{\mathbf{Z}}. \quad (2.3d)$$

The dimensionless parameters are

$$\beta = \frac{K_0 N_0 h^2}{D_C(C_0 - C_{min})}, \quad \gamma = \frac{bV_s}{D_{NO}}, \quad \delta = \frac{D_C}{D_{NO}}, \quad \Gamma = \frac{vN_0gh^3(\rho_c - \rho_w)}{vD_{NO}\rho_w}, \quad Sc = \frac{v}{D_{NO}}, \quad (2.4)$$

where v is the volume of a cell, ρ_c and ρ_w are the densities of a cell and water, respectively, g is the acceleration due to gravity and v is the kinematic viscosity of the fluid. The parameter β represents the strength of oxygen consumption relative to its diffusion, γ is a measure of the relative strengths of directional and random swimming and δ is the ratio of oxygen diffusivity to cell diffusivity. Γ is analogous to the Rayleigh number in thermal convection and Sc is a Schmidt number.

A no-slip condition is imposed at the bottom of the chamber and a stress-free condition at the free surface. The other boundary conditions are: zero vertical component of fluid velocity at the upper and lower boundaries, zero cell flux at all boundaries, zero oxygen flux at the bottom of the chamber and $C = C_0$ at the free surface. These boundary conditions are thus:

at $Z = 0$,

$$\mathbf{U} \cdot \hat{\mathbf{Z}} = 0, \quad \frac{\partial^2}{\partial Z^2}(\mathbf{U} \cdot \hat{\mathbf{Z}}) = 0, \quad \theta = 1, \quad H(\theta) \frac{\partial N}{\partial Z} - \gamma NH(\theta) \frac{\partial \theta}{\partial Z} = 0;$$

at $Z = 1$,

$$\mathbf{U} \cdot \hat{\mathbf{Z}} = 0, \quad \mathbf{U} \times \hat{\mathbf{Z}} = 0, \quad \frac{\partial \theta}{\partial Z} = 0, \quad \frac{\partial N}{\partial Z} = 0.$$

Hillesdon *et al.* (1995) found a steady-state solution in which the fluid velocity is zero and diffusion of cells (random cell swimming) balances chemotaxis (mean swimming up the oxygen gradient), while oxygen diffusion is balanced by oxygen consumption. The steady-state distributions of bacteria (n_0) and oxygen (θ_0) depend only on Z , and whether the chamber is deep or shallow depends on the value of β and γ . If $\beta < (2/\gamma)\sigma \tan^{-1} \sigma$, where $\sigma^2 = e^\gamma - 1$, the chamber is sufficiently shallow that the oxygen concentration is always greater than zero and the steady-state solution is fully analytic. In a deep chamber ($\beta \geq (2/\gamma)\sigma \tan^{-1} \sigma$), the steady-state oxygen concentration is zero below a depth $Z = z_c$ where the value of z_c is found by numerical solution of the initial-value problem. Some chemotactic upswimming occurs before the steady state is set up because the suspension is initially well stirred so that even the bacteria at the bottom of the chamber are active until they have used up all the available oxygen. The total number of cells in the region $0 < Z < z_c$ is $\alpha_c = \int_0^{z_c} n_0 dZ$, which can also be found from solution of the initial-value problem and we expect $z_c \leq \alpha_c < 1$. The deep chamber solution for $0 \leq Z \leq z_c$ is

$$n_0 = \frac{2A_1^2}{\beta\gamma} \sec^2(A_1(z_c - Z)), \quad \theta_0 = 1 - \frac{2}{\gamma} \log \left(\frac{\cos(A_1(z_c - Z))}{\cos A_1 z_c} \right), \quad (2.5)$$

where $A_1 z_c = \tan^{-1} \sigma$ and $\alpha_c = (2\sigma/\beta\gamma z_c) \tan^{-1} \sigma$. For $\beta = 75$, $\gamma = 10$, $\delta = 1$ Hillesdon *et al.* (1995) found $z_c = 0.77$ and $\alpha_c = 0.80$, for example.

In what follows, we will consider only the region in which $\theta > 0$, i.e. $0 < Z < z_c$, and we therefore make a slight alteration to the non-dimensionalization of Hillesdon *et al.* (1995). Instead of using the overall depth of the chamber, h , to non-dimensionalize the depth \tilde{Z} we will use hz_c , the depth of the upper region in which $\theta > 0$. In (2.2) and (2.4), h should therefore be replaced by hz_c . The symbols Z , t , \mathbf{U} , β and Γ now

β	γ	δ	α_c
$\frac{K_0 N_0 h^2 z_c^2}{D_C(C - C_{min})}$	$\frac{bV_s}{D_{N0}}$	$\frac{D_C}{D_{N0}}$	$\int_0^1 n_0 dZ$
45	10	1	1.04

 TABLE 1. Definitions and values of the parameters and α_c for the new non-dimensionalization.

refer to the newly non-dimensionalized quantities (note that β and Γ now involve z_c) and the steady-state distributions are given by

$$n_0 = \frac{2A^2}{\beta\gamma} \sec^2(A(1-Z)), \quad \theta_0 = 1 - \frac{2}{\gamma} \log \left(\frac{\cos(A(1-Z))}{\cos A} \right), \quad (2.6)$$

where $A = \tan^{-1} \sigma$, $A < \frac{1}{2}\pi$ and $\alpha_c = (2\sigma/\beta\gamma) \tan^{-1} \sigma$, where now $\alpha_c = \int_0^1 n_0 dZ$. We will consider only deep chambers where in the new notation $\beta/z_c^2 \geq \frac{2}{\gamma} \sigma \tan^{-1} \sigma$. Table 1 shows the values for the previously mentioned ($\beta = 75$ etc.) steady state from Hillesdon *et al.* (1995), according to the new non-dimensionalization.

3. Axisymmetric upper boundary layer for $\beta\gamma \gg 1$

Hillesdon *et al.* (1995) found that the steady-state cell concentration n_0 has a very thin upper boundary layer containing a high concentration of bacteria when $\beta\gamma \gg 1$ and they developed a boundary-layer scaling in this limit (see Appendix B of that paper). Physically, $\beta\gamma \gg 1$ means that oxygen consumption by the bacteria is large relative to oxygen diffusion from the free surface (large β) and/or that directional cell swimming is strong relative to random cell swimming (large γ). Since we are concerned only with the case in which the cell-rich upper boundary layer (B in figure 2) is narrow, we will only consider the case $\beta\gamma \gg 1$. We assume that the upper boundary layer feeds cells into a narrow falling plume (A).

Hillesdon *et al.* (1995) defined a small parameter λ by

$$\lambda = \frac{2}{\beta\gamma}, \quad (3.1)$$

and scaled the vertical coordinate Z as

$$Z = \lambda z, \quad (3.2a)$$

the horizontal coordinates remaining unchanged. The cell concentration and oxygen concentration were scaled as

$$N = \lambda^{-1} n, \quad \theta = 1 + \frac{2}{\gamma} C. \quad (3.2b)$$

In the absence of fluid motion they found that the steady-state solution is then

$$n = n_0 = \frac{1}{(a+z)^2}, \quad C = c_0 = -\log \left(\frac{a+z}{a} \right), \quad (3.3)$$

for some constant a . In a shallow chamber with no fluid motion, $a = 1$. Rescaling the deep chamber steady-state solution (2.6) in the upper boundary layer gives $a = \alpha_c^{-1}$. The value of α_c given in table 1 gives $a = 0.96$.

We first consider the upper boundary layer, B, in the axisymmetric case. We rewrite the governing equations (2.3a–d) in terms of cylindrical polar coordinates R , ϕ and Z and consider the case where there is no ϕ dependence and no velocity in the ϕ direction so that \mathbf{U} can be written as $(U, 0, W)$. We scale Z , N and θ in the same way as in (3.2a, b) and scale U , W and P as

$$U = U_B u, \quad W = \lambda U_B w, \quad P = P_B p,$$

where U_B and P_B are scaling factors which are as yet unknown.

Using these scalings the axisymmetric governing equations become:

$$\begin{aligned} \lambda^2 U_B \left(u \frac{\partial n}{\partial R} + w \frac{\partial n}{\partial z} \right) + 2n \frac{\partial^2 C}{\partial z^2} + 2 \frac{\partial n}{\partial z} \frac{\partial C}{\partial z} \\ + 2\lambda^2 \left(\frac{n}{R} \frac{\partial C}{\partial R} + n \frac{\partial^2 C}{\partial R^2} + \frac{\partial n}{\partial R} \frac{\partial C}{\partial R} \right) - \frac{\partial^2 n}{\partial z^2} - \lambda^2 \left(\frac{1}{R} \frac{\partial n}{\partial R} + \frac{\partial^2 n}{\partial R^2} \right) = 0, \end{aligned} \quad (3.4a)$$

$$\frac{\partial^2 C}{\partial z^2} - n + \lambda^2 \left(\frac{1}{R} \frac{\partial C}{\partial R} + \frac{\partial^2 C}{\partial R^2} \right) - \frac{\lambda^2}{\delta} U_B \left(u \frac{\partial C}{\partial R} + w \frac{\partial C}{\partial z} \right) = 0, \quad (3.4b)$$

$$\frac{u}{R} + \frac{\partial u}{\partial R} + \frac{\partial w}{\partial z} = 0, \quad (3.4c)$$

$$\lambda^2 U_B S c^{-1} \left(u \frac{\partial u}{\partial R} + w \frac{\partial u}{\partial z} \right) = -\frac{\lambda^2 P_B}{U_B} \frac{\partial p}{\partial R} + \frac{\partial^2 u}{\partial z^2} + \lambda^2 \left(\frac{1}{R} \frac{\partial u}{\partial R} + \frac{\partial^2 u}{\partial R^2} - \frac{u}{R^2} \right), \quad (3.4d)$$

$$\lambda^2 U_B S c^{-1} \left(u \frac{\partial w}{\partial R} + w \frac{\partial w}{\partial z} \right) = -\frac{P_B}{U_B} \frac{\partial p}{\partial z} + \frac{\partial^2 w}{\partial z^2} + \lambda^2 \left(\frac{1}{R} \frac{\partial w}{\partial R} + \frac{\partial^2 w}{\partial R^2} \right) + \frac{\Gamma}{U_B} n. \quad (3.4e)$$

The boundary conditions at $z = 0$ are

$$w = C = \frac{\partial u}{\partial z} = \frac{\partial p}{\partial R} = 0, \quad \frac{\partial n}{\partial z} - 2n \frac{\partial C}{\partial z} = 0.$$

We now expand n , C , u and p in powers of λ :

$$\left. \begin{aligned} n &= n_0 + \lambda n_1 + \cdots, \\ C &= c_0 + \lambda c_1 + \cdots, \\ u &= u_0 + \lambda u_1 + \cdots, \\ p &= p_0 + \lambda p_1 + \cdots, \end{aligned} \right\} \quad (3.5)$$

and assume that $\lambda^2 U_B \ll 1$ so that advection is unimportant at leading order, cell diffusion is balanced by directional cell swimming and oxygen diffusion is balanced by oxygen consumption. Leading order in (3.4a) and (3.4b) gives

$$2n_0 \frac{\partial^2 c_0}{\partial z^2} + 2 \frac{\partial n_0}{\partial z} \frac{\partial c_0}{\partial z} - \frac{\partial^2 n_0}{\partial z^2} = 0, \quad (3.6a)$$

$$\frac{\partial^2 c_0}{\partial z^2} - n_0 = 0. \quad (3.6b)$$

These equations have the solution n_0 and c_0 given in (3.3) but a may now be a function of R .

If $U_B \lambda^2 S c^{-1} \ll 1$, we can neglect fluid momentum, and the leading-order terms in

(3.4d) and (3.4e) are

$$-\frac{\lambda^2}{U_B} P_B \frac{\partial p_0}{\partial R} + \frac{\partial^2 u_0}{\partial z^2} = 0, \quad (3.6c)$$

$$-\frac{P_B}{U_B} \frac{\partial p_0}{\partial z} + \frac{\partial^2 w_0}{\partial z^2} + \frac{\Gamma}{U_B} n_0 = 0. \quad (3.6d)$$

There are three cases to consider here.

If $\Gamma/U_B \gg \lambda^{-2}$, equation (3.6d) requires that we scale $P_B = O(\Gamma)$ so that the pressure term balances the buoyancy term. The pressure term in (3.6c) then dominates to give

$$\frac{\partial p_0}{\partial R} = 0. \quad (3.7)$$

Differentiating (3.6d) with respect to R and using (3.7) gives

$$\frac{\partial n_0}{\partial R} = 0,$$

therefore a must be a constant.

If $\Gamma/U_B = O(\lambda^{-2})$, we again scale P_B as $P_B = O(\Gamma)$. Now the pressure and diffusion terms balance in equation (3.6c) to give

$$\frac{\partial p_0}{\partial R} = \frac{\partial^2 u_0}{\partial z^2}. \quad (3.8)$$

Differentiating (3.6d) with respect to R and using (3.3) and (3.8) to substitute for n_0 and $\partial p_0/\partial R$ gives

$$\frac{\partial^3 u_0}{\partial z^3} = \frac{-2a'}{(a+z)^3},$$

where $a' = \partial a/\partial R$. Integrating this three times with respect to z and applying the boundary conditions on $\partial p_0/\partial R$ and $\partial u_0/\partial z$ at $z = 0$ gives

$$u_0 = -a' \log(a+z) - \frac{a'}{2a^2} z^2 + \frac{a'}{a} z + f(R).$$

This has $u_0 \rightarrow \infty$ at the edge of the upper layer, which is unphysical, unless $a' = 0$. Therefore in this case we must again have a constant and in addition $u_0 = u_0(R)$.

The third case is $1 \ll \Gamma/U_B \ll \lambda^{-2}$. Again, we scale $P_B = O(\Gamma)$ and the diffusion term dominates in equation (3.6c) to give

$$\frac{\partial^2 u_0}{\partial z^2} = 0.$$

Integrating this twice with respect to z and applying the boundary condition on $\partial u/\partial z$ at $z = 0$ gives $u = u_0(R)$, but in this case a may also be a function of R .

In both the last two cases the function $u_0(R)$ cannot be found from the boundary-layer equations alone. It will be determined only by matching to the outer zone, C.

4. Axisymmetric plumes

4.1. Scaling

In the plume, we scale the radial coordinate as

$$R = \epsilon r, \quad (4.1a)$$

where $0 < \epsilon \ll 1$. The vertical coordinate remains Z . We also scale the cell concentration, the oxygen concentration, the vertical and horizontal fluid velocity and the pressure as

$$N = N_A n, \quad \theta = 1 + C_A C, \quad W = W_A w, \quad U = \epsilon W_A u, \quad P = P_A p, \quad (4.1b)$$

where N_A , C_A , W_A and P_A are scaling factors which are as yet unknown. Using this scaling and neglecting terms which are obviously $O(\epsilon^2)$, the axisymmetric governing equations become

$$\epsilon^2 W_A \left(u \frac{\partial n}{\partial r} + w \frac{\partial n}{\partial Z} \right) + \gamma C_A \left(\frac{\partial n}{\partial r} \frac{\partial C}{\partial r} + \frac{n}{r} \frac{\partial C}{\partial r} + n \frac{\partial^2 C}{\partial r^2} \right) = \frac{\partial^2 n}{\partial r^2} + \frac{1}{r} \frac{\partial n}{\partial r}, \quad (4.2a)$$

$$\frac{\epsilon^2 W_A}{\delta} \left(u \frac{\partial C}{\partial r} + w \frac{\partial C}{\partial Z} \right) + \frac{\epsilon^2 \beta N_A}{C_A} n = \frac{\partial^2 C}{\partial r^2} + \frac{1}{r} \frac{\partial C}{\partial r}, \quad (4.2b)$$

$$\frac{u}{r} + \frac{\partial u}{\partial r} + \frac{\partial w}{\partial Z} = 0, \quad (4.2c)$$

$$\epsilon^2 W_A S c^{-1} \left(u \frac{\partial u}{\partial r} + w \frac{\partial u}{\partial Z} \right) = -\frac{P_A}{W_A} \frac{\partial p}{\partial r} + \frac{\partial^2 u}{\partial r^2} + \frac{1}{r} \frac{\partial u}{\partial r} - \frac{u}{r^2}, \quad (4.2d)$$

$$\epsilon^2 W_A S c^{-1} \left(u \frac{\partial w}{\partial r} + w \frac{\partial w}{\partial Z} \right) = -\epsilon^2 \frac{P_A}{W_A} \frac{\partial p}{\partial Z} + \epsilon^2 \frac{N_A}{W_A} \Gamma n + \frac{\partial^2 w}{\partial r^2} + \frac{1}{r} \frac{\partial w}{\partial r}. \quad (4.2e)$$

The scaling factors N_A , C_A , W_A and P_A are chosen so that the appropriate terms are retained in (4.2a–e). In order to retain the advection terms, we scale $W_A = \epsilon^{-2}$, and in order to retain the chemotaxis terms, we let $C_A = 2/\gamma$ (compare equation (3.2b)). The oxygen consumption term in (4.2b) is therefore $(\epsilon^2 \beta \gamma / 2) N_A n = (\epsilon^2 / \lambda) N_A n$, where λ is defined in (3.1). In order to retain this term we let $N_A = \lambda / \epsilon^2$. Using these scalings the buoyancy term $\epsilon^2 (N_A / W_A) \Gamma n$ in equation (4.2e), which must be important because it drives the whole flow, will be retained only if $\Gamma = O(\lambda^{-1} \epsilon^{-2})$. We therefore write $\Gamma = \lambda^{-1} \epsilon^{-2} \tilde{\Gamma}$, where $\tilde{\Gamma}$ is $O(1)$. Finally, in order to keep the pressure term in (4.2e), we must scale $P_A = \epsilon^{-4}$. The leading term in (4.2d) is therefore $\partial p / \partial r = 0$, hence $p = p(Z)$.

Substituting for N_A , C_A and W_A in (4.2a, b) we obtain

$$u \frac{\partial n}{\partial r} + w \frac{\partial n}{\partial Z} + 2 \frac{\partial n}{\partial r} \frac{\partial C}{\partial r} + 2 \frac{n}{r} \frac{\partial C}{\partial r} + 2n \frac{\partial^2 C}{\partial r^2} - \frac{1}{r} \frac{\partial n}{\partial r} - \frac{\partial^2 n}{\partial r^2} = 0, \quad (4.3a)$$

$$\frac{1}{\delta} \left(u \frac{\partial C}{\partial r} + w \frac{\partial C}{\partial Z} \right) + n - \left(\frac{1}{r} \frac{\partial C}{\partial r} + \frac{\partial^2 C}{\partial r^2} \right) = 0. \quad (4.3b)$$

Differentiating (4.2e) with respect to r and substituting for N_A , W_A and Γ gives

$$S c^{-1} \left(\frac{\partial u}{\partial r} \frac{\partial w}{\partial r} + u \frac{\partial^2 w}{\partial r^2} + \frac{\partial w}{\partial r} \frac{\partial w}{\partial Z} + w \frac{\partial^2 w}{\partial r \partial Z} \right) = \tilde{\Gamma} \frac{\partial n}{\partial r} + \frac{\partial^3 w}{\partial r^3} + \frac{1}{r} \frac{\partial^2 w}{\partial r^2} - \frac{1}{r^2} \frac{\partial w}{\partial r}. \quad (4.3c)$$

We impose the following boundary conditions on these equations. Symmetry about $r = 0$ requires at $r = 0$:

$$\frac{\partial n}{\partial r} = 0, \quad \frac{\partial C}{\partial r} = 0, \quad u = 0, \quad \frac{\partial w}{\partial r} = 0.$$

As $r \rightarrow \infty$ we impose:

$$n \rightarrow 0, \quad \frac{\partial C}{\partial r} \rightarrow 0, \quad w \rightarrow 0.$$

4.2. Similarity solution

We now seek a similarity solution to equations (4.3a–c). We let h be the width of the plume and pose a solution of the form

$$h \propto Z^a, \quad w \propto Z^b, \quad n \propto Z^c, \quad C \propto Z^d, \quad u \propto Z^{a+b-1}. \quad (4.4)$$

Substituting this solution into equations (4.3) and equating the powers of Z gives $a = \frac{1}{2}$, $b = 0$, $c = -1$, $d = 0$. Since the plume width, h , is proportional to $Z^{1/2}$ we define a similarity variable

$$\eta = \frac{r}{Z^{1/2}}, \quad (4.5)$$

and pose a solution

$$n = Z^{-1}H(\eta), \quad C = G(\eta), \quad \psi = ZF(\eta), \quad u = Z^{-1/2} \left(\frac{F}{\eta} - \frac{F'}{2} \right), \quad w = -\frac{F'}{\eta}, \quad (4.6)$$

where ψ is the streamfunction and primes denote differentiation with respect to η . This similarity solution is similar to that given for a thermal plume rising from an isolated point source of heat by Yih (1951) in which the plume width is proportional to $Z^{1/2}$ and the streamfunction is proportional to Z .

Substituting this solution into equation (4.3a), integrating once with respect to η and applying the boundary conditions at $\eta = 0$ gives

$$HF + 2\eta HG' - \eta H' = 0. \quad (4.7a)$$

Substituting into equation (4.3b) gives

$$\eta G'' + G' - \frac{1}{\delta} G' F - \eta H = 0, \quad (4.7b)$$

and substituting into (4.3c), integrating the resulting equation once with respect to η and applying the boundary conditions as $\eta \rightarrow \infty$ gives

$$\frac{1}{\eta} F''' - \frac{1}{\eta^2} F'' + \frac{1}{\eta^3} F' + Sc^{-1} \left(\frac{1}{\eta^3} FF' - \frac{1}{\eta^2} FF'' \right) - \tilde{T} H = 0. \quad (4.7c)$$

The boundary conditions are:

at $\eta = 0$:

$$H' = G' = \frac{F}{\eta} - \frac{F'}{2} = \frac{F'}{\eta^2} - \frac{F''}{\eta} = 0$$

as $\eta \rightarrow \infty$:

$$H \rightarrow 0, \quad G' \rightarrow 0, \quad \frac{F'}{\eta} \rightarrow 0.$$

4.3. Cell and fluid fluxes in the plume

Equation (4.3a) can be written as

$$\frac{1}{r} \frac{\partial}{\partial r} \left(rnu + 2rn \frac{\partial C}{\partial r} - r \frac{\partial n}{\partial r} \right) + \frac{\partial}{\partial Z} (nw) = 0.$$

Multiplying this by r , integrating from zero to infinity with respect to r and applying the boundary conditions at $r = 0, \infty$ gives

$$\frac{\partial}{\partial Z} \int_0^\infty nwr \, dr = 0, \quad (4.8)$$

hence the dimensionless cell flux in the plume, $\int_0^\infty nwr \, dr$, is independent of Z . We will denote this constant cell flux by Q . In terms of the similarity solution

$$Q = \int_0^\infty -HF' \, d\eta. \quad (4.9)$$

The total fluid flux in the plume is given by

$$\epsilon^2 W_0 \int_0^\infty wr \, dr = Z \int_0^\infty -F' \, d\eta.$$

The boundary condition $F'/\eta \rightarrow 0$ as $\eta \rightarrow \infty$ (i.e. $w \rightarrow 0$ as $r \rightarrow \infty$) gives $F \rightarrow -M$ as $\eta \rightarrow \infty$, where M is a constant. Using this boundary condition and $F = 0$ at $\eta = 0$ gives

$$\epsilon^2 W_0 \int_0^\infty wr \, dr = MZ. \quad (4.10)$$

The fluid flux in the plume increases with depth, therefore the plume must be entraining fluid from the region outside the plume. The horizontal fluid velocity in the plume is given in (4.6). As $\eta \rightarrow \infty$ the boundary conditions $F'/\eta \rightarrow 0$ and $F \rightarrow -M$ give $u \rightarrow -MZ^{-1/2}\eta^{-1}$. Using the definition of η we therefore have that as $\eta \rightarrow \infty$

$$u \rightarrow -\frac{M}{r}. \quad (4.11)$$

We expect a plume solution to exist for each value of the cell flux, Q , and the value of Q will therefore determine the value of M . Later we find Q by coupling regions A and B to C.

Note that in the case of thermal convection from a point source (Yih 1951) the condition that the heat flux in the plume is constant (the equivalent to 4.8) introduces an extra condition which allows a similarity solution to be found. Here, a similarity solution can be obtained from the equations alone and this similarity solution does satisfy the condition (4.8). Alternatively, we can say that the similarity solution must satisfy (4.8) and that in three dimensions the addition of the chemotaxis and oxygen consumption terms to the plume equations does not alter the form of the similarity solution.

4.4. Analytic solutions for $\gamma = 0$

In general equations (4.7a–c) for H , G' and F must be solved numerically. It is, however, possible to find an analytic solution when $\gamma = 0$, i.e. when chemotaxis is unimportant in the plume itself, for particular values of the other parameters. In this case, the scaling in equations (4.2a–e) is slightly different. We will assume that $\beta = O(1)$. When $\gamma = 0$ we scale W_0 and P_0 as before but we have $C_0 = 1$, $N_0 = \epsilon^{-2}$ and we write $\Gamma = \epsilon^{-2}\tilde{\Gamma}$. Using these scalings and the similarity solution of (4.6) equations (4.7a, b) become

$$\eta G'' + G' - \frac{1}{\delta} G' F - \eta H = 0, \quad (4.12a)$$

$$HF - \eta H' = 0. \quad (4.12b)$$

Equation (4.7c) is unchanged.

For the problem of thermal convection from a point source of heat, analytic solutions can be obtained when the Prandtl number (equivalent to the Schmidt number in bioconvection) takes the values 1 or 2 (Yih 1951). Following Yih (1951),

we find four analytic solutions

$$\begin{aligned}
 Sc = 1, \delta = 1 : F &= \frac{-6A\eta^2}{1 + A\eta^2}, & H &= \frac{96A^2}{\tilde{\Gamma}(1 + A\eta^2)^3}, & G' &= \frac{48\beta A^2\eta}{\tilde{\Gamma}(1 + A\eta^2)^3}, \\
 Sc = 1, \delta = \frac{3}{4} : F &= \frac{-6A\eta^2}{1 + A\eta^2}, & H &= \frac{96A^2}{\tilde{\Gamma}(1 + A\eta^2)^3}, & G' &= \frac{24\beta A^2(A\eta^3 + 2\eta)}{\tilde{\Gamma}(1 + A\eta^2)^4}, \\
 Sc = 2, \delta = 1 : F &= \frac{-8A\eta^2}{1 + A\eta^2}, & H &= \frac{128A^2}{\tilde{\Gamma}(1 + A\eta^2)^4}, & G' &= \frac{64\beta A^2\eta}{\tilde{\Gamma}(1 + A\eta^2)^4}, \\
 Sc = 2, \delta = 2 : F &= \frac{-8A\eta^2}{1 + A\eta^2}, & H &= \frac{128A^2}{\tilde{\Gamma}(1 + A\eta^2)^4}, & G' &= \frac{64\beta A^2\eta}{\tilde{\Gamma}(1 + A\eta^2)^3}.
 \end{aligned}$$

All these solutions satisfy the boundary conditions at $\eta = 0$ and as $\eta \rightarrow \infty$. The value of A is set by the condition $\int_0^\infty HF' d\eta = -Q$. For $Sc = 1$ and $\delta = 1$ or $\frac{3}{4}$ this gives $A^2 = Q\tilde{\Gamma}/144$ and for $Sc = 2$ and $\delta = 1$ or 2 it gives $A^2 = 5Q\tilde{\Gamma}/1024$. These analytic solutions can be used to check the numerical solution and also as a starting point for it.

4.5. Series expansion for $\eta \ll 1$

Equations (4.7a-c) are singular at $\eta = 0$ and therefore cannot be solved numerically over the entire range of η . However, a series expansion for $\eta \ll 1$ can be used to start the numerical solution away from $\eta = 0$. For $\eta \ll 1$, we pose an expansion of the form

$$\begin{aligned}
 H &= h_0 + \eta h_1 + \eta^2 h_2 + \eta^3 h_3 + \eta^4 h_4 + \eta^5 h_5 + \dots, \\
 G' &= g_0 + \eta g_1 + \eta^2 g_2 + \eta^3 g_3 + \eta^4 g_4 + \eta^5 g_5 + \dots, \\
 F &= f_0 + \eta f_1 + \eta^2 f_2 + \eta^3 f_3 + \eta^4 f_4 + \eta^5 f_5 + \dots.
 \end{aligned}$$

In order to satisfy the boundary conditions at $\eta = 0$ we require

$$h_1 = g_0 = f_0 = f_1 = f_3 = 0,$$

but we require $h_0 \neq 0$ in order to have a non-zero cell concentration at $\eta = 0$ and $f_2 \neq 0$ in order to have $w \neq 0$ at $\eta = 0$. A solution can be found in terms of the two constants h_0 and f_2 as follows:

$$h_2 = \frac{2h_0^2}{4} + \frac{h_0 f_2}{2}, \quad (4.13a)$$

$$h_4 = \frac{3}{16}h_0^3 + \frac{5}{16}h_0^2 f_2 + \frac{1}{16\delta}h_0^2 f_2 + \frac{h_0 f_2^2}{8} + \frac{h_0^2 \tilde{\Gamma}}{64}, \quad (4.13b)$$

$$g_1 = \frac{1}{2}h_0, \quad (4.13c)$$

$$g_3 = \frac{1}{8\delta}h_0 f_2 + \frac{1}{8}h_0^2 + \frac{1}{8}h_0 f_2, \quad (4.13d)$$

$$f_4 = \frac{h_0 \tilde{\Gamma}}{16}, \quad (4.13e)$$

$$f_6 = \frac{1}{192}h_0^2 \tilde{\Gamma} + \frac{h_0 f_2 \tilde{\Gamma}}{192}(1 + Sc^{-1}), \quad (4.13f)$$

$$h_3 = g_2 = g_4 = f_5 = f_7 = 0. \quad (4.13g)$$

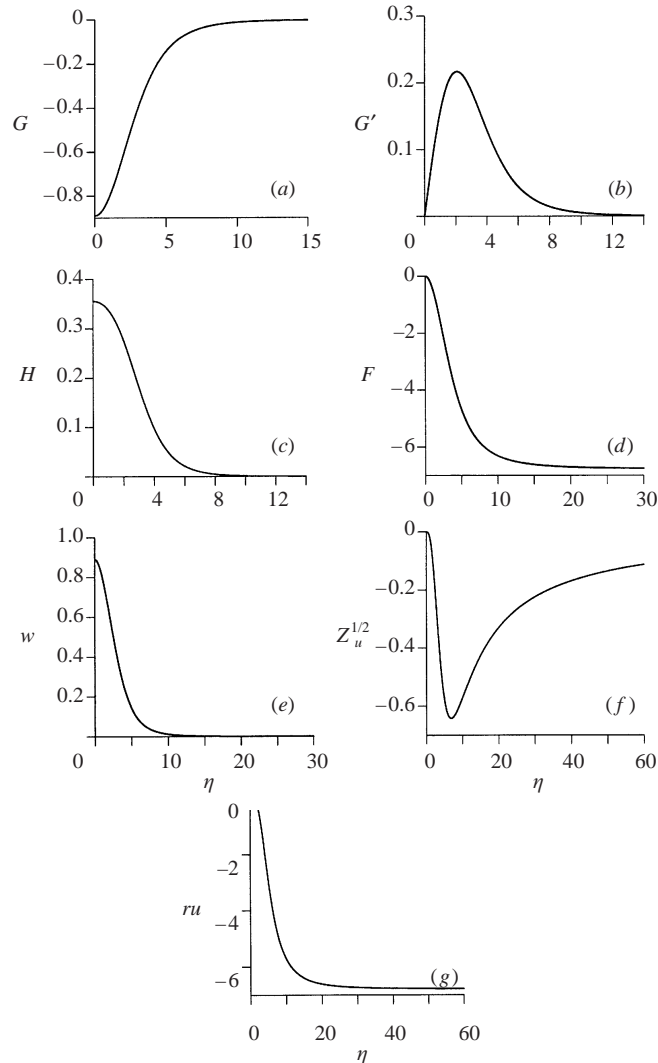


FIGURE 3. Graphs of G , G' , H , F , $w = -F'/\eta$, $Z^{1/2}u = F/\eta - \frac{1}{2}F'$ and $ru = F - \frac{1}{2}\eta F'$ for an axisymmetric plume. ($\delta = 1$, $Sc = 1$, $\tilde{T} = 1$ and $Q = 1$.)

4.6. Results

The ordinary differential equations (4.7a-c) for H , G' and F are solved numerically subject to the given boundary conditions. We start the solution at $\eta = 0.01$ using the series solution given in §4.5, which depends on the two unknown constants h_0 and f_2 . The method of solution is to treat h_0 and f_2 as variables and introduce them into the system of equations (by adding equations $h'_0 = f'_2 = 0$) and impose the cell flux $Q = -\int_0^\infty HF'$ as a constant of the solution. We therefore have an eighth-order system of ordinary differential equations subject to six boundary conditions at $\eta = 0.01$ and two as $\eta \rightarrow \infty$. This system of equations is solved using the NRK routine (Cash & Moore 1980) which uses finite differences and Newton iterations. We compared the results of the numerical solution with the analytic solution in the case $\beta = O(1)$, $\gamma = 0$ given in §4.4 and with the series expansion for $\eta \ll 1$ given in §4.5 and found that in both cases the numerical solution and the analytic solution agreed.

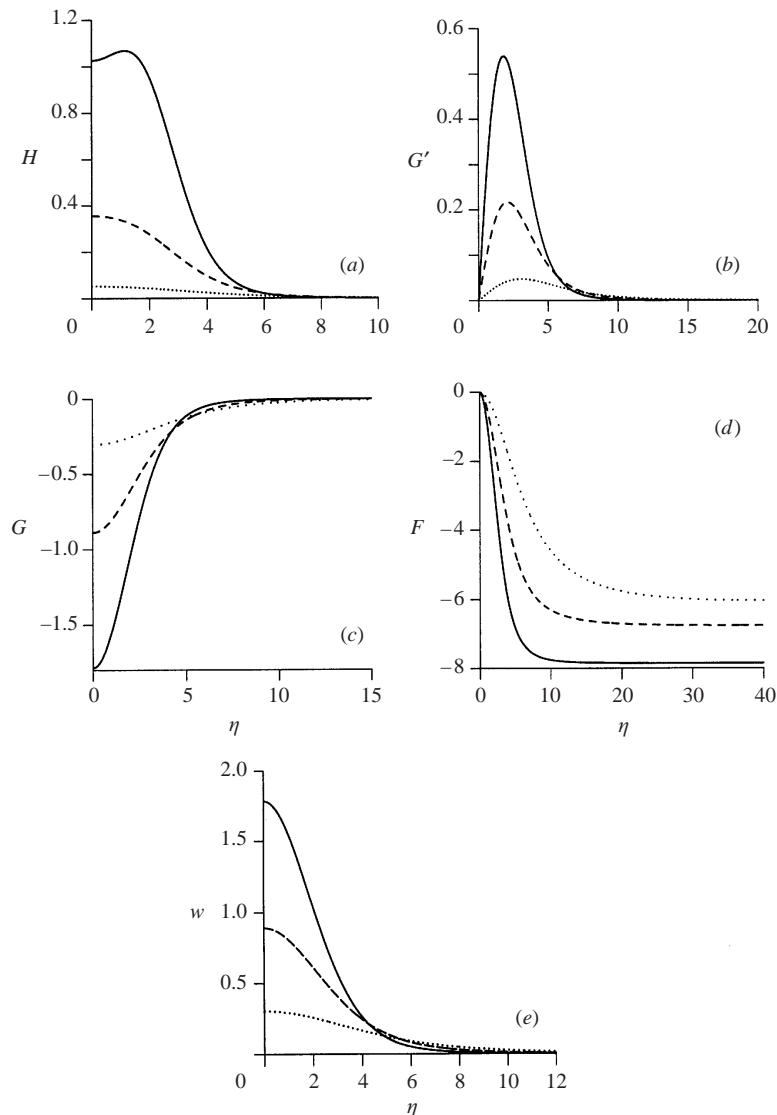


FIGURE 4. Graphs of H , G , G' , F and w for $\delta = 1$, $Sc = 1$, $\tilde{T} = 1$ and $Q = 0.1, 1, 5$.
 \cdots , $Q = 0.1$; $---$, $Q = 1$; $—$, $Q = 5$.

The solution depends on the parameters δ , Sc and \tilde{T} and on the cell flux Q . Figure 3 contains the solutions for $\delta = 1$, $Sc = 1$, $\tilde{T} = 1$ and $Q = 1$. G is calculated by numerical integration of G' and contains an arbitrary constant which we have chosen so that $G = 0$ (i.e. $\theta = 1$) at the edge of the plume. The oxygen concentration is given by $\theta = 1 + (2/\gamma)G(\eta)$ and we will assume that γ is such that θ is always positive so that all the bacteria are active. From figure 3(a), we see that the oxygen concentration inside the plume is lower than that outside, which is reasonable since the plume contains a high concentration of bacteria which consume oxygen. Figures 3(d)–3(g) show that as $\eta \rightarrow \infty$, $F \rightarrow \text{constant}$, so $w \rightarrow 0$ and $ru \rightarrow \text{constant}$, as required by the boundary conditions. Calling this constant $-M$ (as in (4.11)), we find that in this case $M = 6.79$.

We first considered fixed values of δ , Sc and \tilde{T} and varied the value of the cell flux

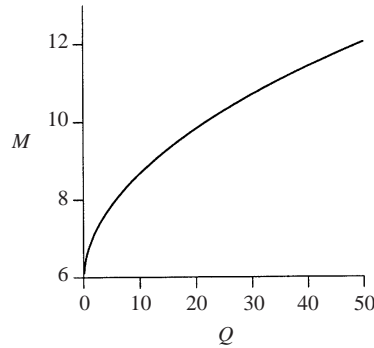


FIGURE 5. Graph of fluid flux into the plume, M , against cell flux downwards in the plume, Q , for an axisymmetric plume. ($\delta = 1$, $Sc = 1$, $\tilde{\Gamma} = 1$).

Q . Figure 4 shows graphs of H , G , G' , F and w for $\delta = 1$, $Sc = 1$, $\tilde{\Gamma} = 1$ and $Q = 0.1$, 1 and 5. As we would expect, the cell concentration in the plume is greater for higher values of Q but the width of the plume decreases slightly. The higher concentration of cells leads to a greater consumption of oxygen so that the oxygen concentration at the centre of the plume decreases. As the cell flux increases, the vertical fluid velocity, w , at the centre of the plume increases and the value of M increases, indicating that the horizontal fluid flow into the plume increases. Figure 5 is a graph of the fluid flux into the plume, M , against the cell flux downwards in the plume, Q .

Figure 6 shows solutions for $\delta = 1$, $\tilde{\Gamma} = 1$, $Q = 1$ and $Sc = 0.2$, 1 and 5. From these graphs we can see that as Sc increases the cell concentration in the centre of the plume increases but the cell profile becomes narrower and the total number of cells in the plume decreases. The oxygen concentration in the plume is therefore higher and the oxygen profile is also narrower. The fluid velocity w in the centre of the plume increases as Sc increases, therefore the total cell flux is the same. At large values of Sc the velocity is non-zero over a much larger range than the cell and oxygen concentrations, indicating that the plume has a two-layer structure similar to that found in thermal convection at large Prandtl number (Kuiken & Rotem 1971; Worster 1986).

Figure 7 shows solutions for $\delta = 1$, $Sc = 1$, $Q = 1$ and $\tilde{\Gamma} = 0.2$, 1 and 5. When $\tilde{\Gamma}$ is large the effect of buoyancy is important. As $\tilde{\Gamma}$ increases, the cell concentration in the centre of the plume increases, but the plume becomes narrower, so the total number of cells at any Z decreases. Therefore the oxygen profile becomes narrower and the oxygen concentration in the centre of the plume increases. The fluid velocity w in the centre of the plume is larger for large values of $\tilde{\Gamma}$, because the force of buoyancy is more important, but w falls to zero more rapidly than for small $\tilde{\Gamma}$. M decreases as $\tilde{\Gamma}$ increases, indicating that less fluid is entrained by the plume.

Figure 8 shows solutions for $\tilde{\Gamma} = 1$, $Sc = 1$, $Q = 1$ and $\delta = 0.2$, 1 and 5. $\delta = D_C/D_{N_0}$, therefore a large value of δ corresponds to a large value of oxygen diffusion relative to cell diffusion. As δ increases, inward chemotaxis takes place over a wider area and the plume becomes wider. The cell concentration and the fluid velocity w decrease in the centre of the plume. Increasing δ for fixed β makes the oxygen consumption per cell greater, therefore the value of G at the centre of the plume decreases. For $\delta = 5$, the oxygen gradient, G' , is non-zero over a much wider area than either the cell concentration, H , or the vertical fluid velocity, w .

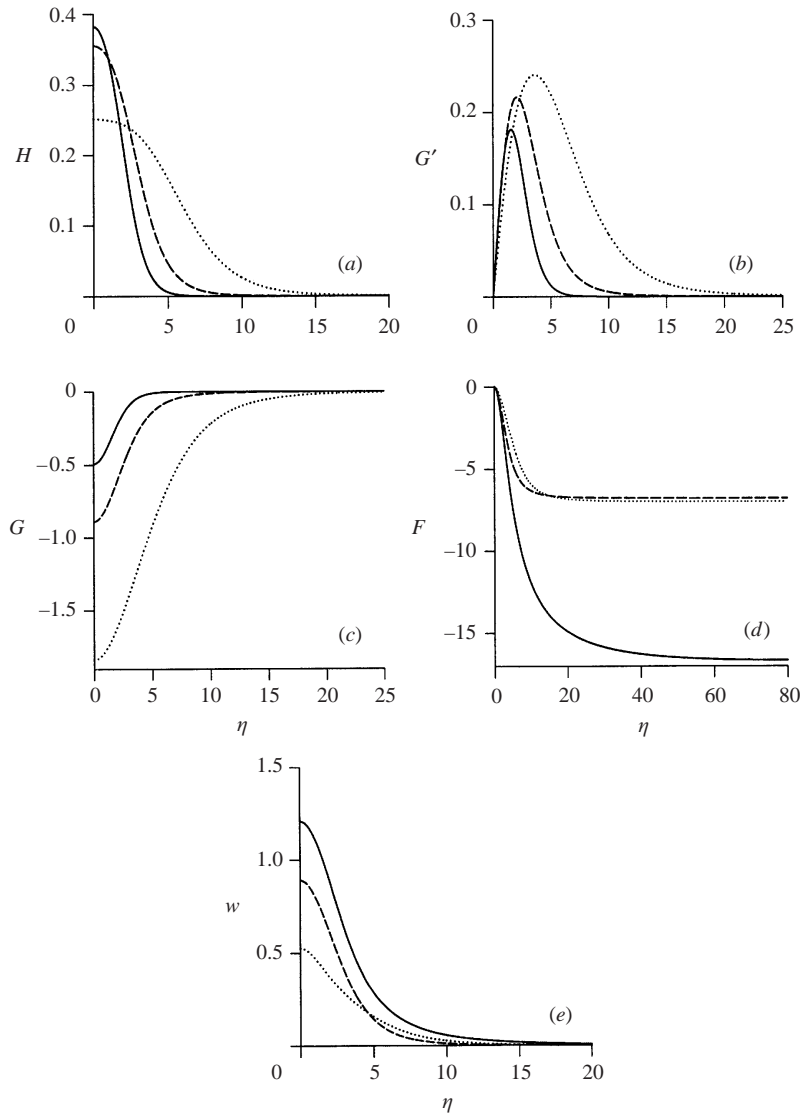


FIGURE 6. Graphs of H , G , G' , F and w for $\delta = 1$, $Q = 1$, $\tilde{F} = 1$ and $Sc = 0.2, 1, 5$.
 \cdots , $Sc = 0.2$; $---$, $Sc = 1$; $---$, $Sc = 5$.

5. Axisymmetric outer flow

The descending plume of fluid entrains fluid from the outer region and therefore drives a fluid motion there. The cell concentration is negligible in this outer region, since all the bacteria have swum up into the upper boundary layer, therefore the effect of buoyancy is negligible. If the Schmidt number is large or the flow is slow, the governing equations in this outer region are the continuity equation and the Stokes equations:

$$\nabla P = \nabla^2 U. \quad (5.1)$$

We will solve these equations in the outer region $0 < Z < 1$, $b < R < d$, where $R = d$ is the outer boundary and $R = b$ is a constant, taken to represent the edge of the

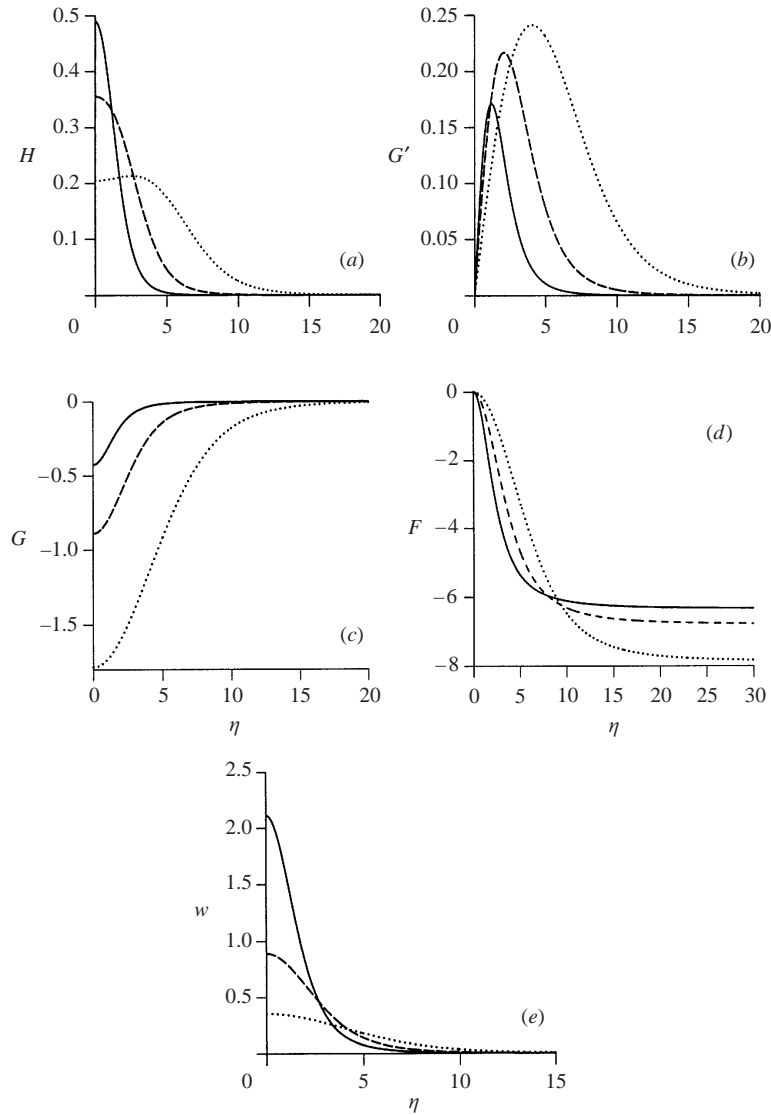


FIGURE 7. Graphs of H , G , G' , F and w for $\delta = 1$, $Q = 1$, $Sc = 1$ and $\tilde{\Gamma} = 0.2, 1, 5$.
 \cdots , $\tilde{\Gamma} = 0.2$; $---$, $\tilde{\Gamma} = 1$; $---$, $\tilde{\Gamma} = 5$.

plume. We will let $b \rightarrow 0$ later. U is written in terms of a stream function ψ and we impose stress-free boundary conditions at the upper and lower surfaces: at $Z = 0, 1$

$$\frac{\partial \psi}{\partial R} = \frac{\partial^2 \psi}{\partial Z^2} = 0. \quad (5.2a)$$

At the outer boundary $R = d$, we impose $U = \partial W / \partial R = 0$:

$$\frac{\partial \psi}{\partial Z} = 0, \quad -\frac{1}{R} \frac{\partial^2 \psi}{\partial R^2} + \frac{1}{R^2} \frac{\partial \psi}{\partial R} = 0. \quad (5.2b)$$

The boundary conditions at the edge of the plume ($R = b$) are set by the similarity solution in the plume. The vertical fluid velocity in the plume, w , tends to zero at

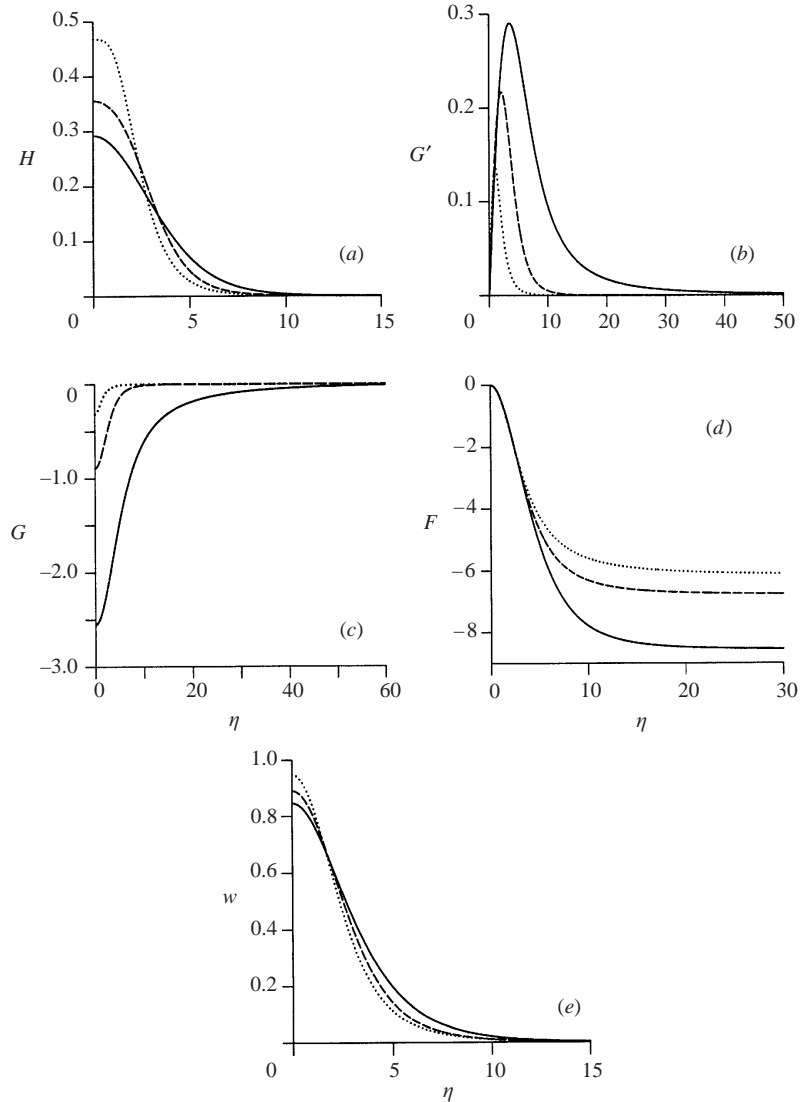


FIGURE 8. Graphs of H , G , G' , F and w for $\tilde{\Gamma} = 1$, $Q = 1$, $Sc = 1$ and $\delta = 0.2, 1, 5$.
 \cdots , $\delta = 0.2$; $---$, $\delta = 1$; $---$, $\delta = 5$.

the edge of the plume. Since $W = \epsilon^{-2}w$, this boundary condition can be satisfied by requiring that either W is finite at $R = b$ or $W = 0$ at $R = b$. Which of these two possibilities holds depends on the higher-order solutions in the plume. In either case we require

$$-\frac{1}{R} \frac{\partial \psi}{\partial R} = \text{constant} \quad (5.2c)$$

at $R = b$, and the constant may be zero.

The plume entrains fluid from the outer region and at the edge of the plume $ru = -M$, which is $RU = -M$ in the unscaled outer variables. Conservation of mass shows that this uniform inflow cannot persist all the way to the bottom of the

chamber. We could instead postulate a lower boundary Z_L of the zone of interest at which, outside the plume, there is an upflow equal in flow rate to the downflow, $\pi M Z_L$, in the plume at that level. Alternatively, since we are most interested in the solution in the upper part of the fluid, we could postulate that $RU = -M$ at $r = b$ in the upper part of the plume with a corresponding outflow in the lower part. We choose the latter; the exact form of this boundary condition in the lower part is unimportant. The similarity solution in the plume may not be valid throughout the entire depth of fluid anyway, a possibility which will be more fully discussed later. Thus, we take the boundary condition at the inner boundary $R = b$ to be

$$\frac{\partial \psi}{\partial Z} = \tilde{\alpha}, \quad (5.2d)$$

where $\tilde{\alpha}$ is equal to $-M$ for $0 < Z < 0.75$ and then increases smoothly so that $\int_0^1 U dZ = 0$, to ensure conservation of fluid. We choose

$$\tilde{\alpha} = \begin{cases} -M & \text{for } 0 < Z < 0.75, \\ 2560M(Z - 0.75)^3 - 7680M(Z - 0.75)^4 - M & \text{for } 0.75 < Z < 1. \end{cases} \quad (5.3)$$

Taking the curl of (5.1) gives

$$D^2 D^2 \psi = 0, \quad (5.4)$$

where the differential operator is

$$D^2 = \frac{\partial^2}{\partial R^2} - \frac{1}{R} \frac{\partial}{\partial R} + \frac{\partial^2}{\partial Z^2}.$$

We pose a separable solution of the form

$$\psi = f(R)g(Z),$$

where $\partial^2 g / \partial Z^2 \propto g$. In the light of the boundary conditions (5.2a) on $Z = 0, 1$ we will choose $\partial^2 g / \partial Z^2 = -k^2 g$ so that $g(Z) = \sin(kZ)$, where $k = n\pi$ and $n = 1, 2, 3, \dots$. We find that the solution for f is

$$f = AR I_1(kR) + BR^2 I_1'(kR) + CR K_1(kr) + DR^2 K_1'(kR),$$

where I_1 and K_1 are modified Bessel functions, the primes denote $(1/k)(\partial/\partial R)$ and A, B, C and D are arbitrary constants. The general solution to (5.4) satisfying (5.2a) is thus

$$\psi = \sum_n \sin(n\pi Z) (A_n R^2 I_1'(n\pi R) + B_n R I_1(n\pi R) + C_n R^2 K_1'(n\pi R) + D_n R K_1(n\pi R)).$$

The constants A_n, B_n, C_n and D_n are chosen so that the boundary conditions at $R = b, d$ are satisfied.

If the constant in (5.2c) is non-zero, these have the solution

$$A_n = \frac{1}{2} n^2 \pi^2 \alpha_n \lambda_n + O((\log(\frac{1}{2} n\pi b))^{-1}), \quad (5.5a)$$

$$B_n = -\frac{1}{2} n\pi \alpha_n \lambda_n (1 + n\pi p_n) + O((\log(\frac{1}{2} n\pi b))^{-1}), \quad (5.5b)$$

$$C_n = -\frac{1}{2} n^2 \pi^2 \alpha_n + O((\log(n\pi b))^{-1}), \quad (5.5c)$$

$$D_n = \frac{1}{2} n\pi \alpha_n + O((\log(\frac{1}{2} n\pi b))^{-1}), \quad (5.5d)$$

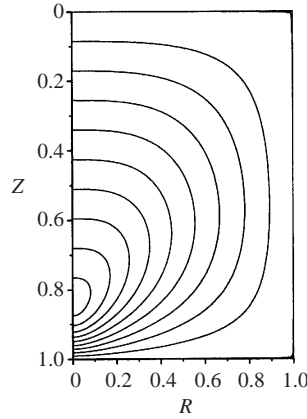


FIGURE 9. Streamlines for axisymmetric outer flow when $M = 6.79$, $d = 1$.

where

$$\alpha_n = \frac{61\,440M}{n^5\pi^5} \cos(n\pi) + \frac{30\,720M}{n^5\pi^5} \cos\left(\frac{3}{4}n\pi\right) + \frac{368\,640M}{n^6\pi^6} \sin\left(\frac{3}{4}n\pi\right),$$

$$\lambda_n = \frac{K_1(n\pi d)}{I_1(n\pi d)}, \quad p_n = (n\pi I_1(n\pi d)K_1(n\pi d))^{-1}.$$

(If the constant in (5.2c) is zero, the leading terms are unaltered, only the higher-order terms change.) The $(\log(\frac{1}{2}n\pi b))^{-1}$ terms arise from the series expansion of K_1 for small b (see Metcalfe 1998 for full details).

These coefficients can be used to plot streamlines of the axisymmetric outer flow. Figure 9 shows the streamlines calculated using the values of the coefficients given in (5.5a–d), i.e. when the constant in (5.2c) is non-zero, when $d = 1$ and $M = 6.79$, the value of M corresponding to the graphs of figure 3. The streamlines in the figure were calculated using the first twenty and the first forty terms of the series and they lie on top of each other.

6. Matching the axisymmetric solutions in different regions in the limit $\beta\gamma \gg 1$

So far we have modelled the deep chamber experiments of figure 1 in three separate regions: an upper boundary layer of depth λ , a falling plume of width ϵ and the region outside the plume. In §3, we found a solution for the cell and oxygen concentrations and the fluid velocity in the upper boundary layer. This solution depends on the size of the Rayleigh number, Γ , and the scaling for the horizontal fluid velocity, U_B . In §4, we derived a similarity solution in the falling plume and in §5 we found a solution for the flow in the outer region driven by the falling plume. We now match the solutions in these different regions. We are considering the limit $\beta\gamma \gg 1$, as it is only in this limit that an upper boundary layer forms.

In the outer region, the horizontal fluid velocity is given by

$$U = \sum_n n\pi \cos(n\pi Z) [A_n R I_1'(n\pi R) + B_n I_1(n\pi R) + C_n R K_1'(n\pi R) + D_n K_1(n\pi R)]. \quad (6.1)$$

At the edge of the upper boundary layer, $Z = \lambda$, this is

$$U = \sum_n n\pi[A_n R I_1'(n\pi R) + B_n I_1(n\pi R) + C_n R K_1'(n\pi R) + D_n K_1(n\pi R)] + O(\lambda^2), \quad (6.2)$$

which indicates that the horizontal fluid velocity in the upper layer is $O(1)$. We therefore require

$$U_B = 1, \quad (6.3)$$

and $u_0(R)$ (§3) is given by (6.2). We will write $u_{0\epsilon} = u_0(R = \epsilon)$ for the fluid velocity in the upper layer at the edge of the plume $R = \epsilon$. Equation (6.2) gives

$$u_{0\epsilon} = \frac{1}{\epsilon} \sum_n n\pi\alpha_n. \quad (6.4)$$

We do not consider in detail the turning region in which the inward flow of cells in the boundary layer is converted into the falling plume; experience with other boundary layers suggests that the flow here is inviscid and passive (e.g. Lyne 1971). However, the cell flux and the fluid flux between the upper layer and the plume must match. The fluid flux in the plume is given by

$$MZ, \quad (6.5)$$

where M is a constant of $O(1)$. At the top of the plume the fluid flux is therefore $O(\lambda)$. The fluid flux out of the upper boundary layer into the plume is $O(\epsilon\lambda U_B u_{0\epsilon})$. From (6.3) and (6.4) this is $O(\lambda)$, which is consistent with the fluid flux in the plume.

The similarity solution in the plume has constant cell flux

$$\pi\epsilon^2 N_A W_A \int_0^\infty nwr \, dr = \frac{\lambda}{\epsilon^2} \pi Q.$$

The cell flux out of the upper boundary layer into the plume is

$$-2\pi\epsilon\lambda U_B \lambda^{-1} \int_0^\infty n_{0\epsilon} u_{0\epsilon} \, dz,$$

where $n_{0\epsilon} = n_0(R = \epsilon)$. Using (3.3), (6.3) and (6.4), this cell flux is

$$-\frac{2\pi}{a} \sum_n n\pi\alpha_n,$$

which is $O(1)$ if a is $O(1)$. This is consistent with the cell flux in the plume only if

$$\lambda = \epsilon^2, \quad (6.6)$$

thus determining ϵ in terms of λ . Moreover, for the two cell fluxes to be equal we must have

$$Q = \frac{2}{a} \sum_n n\pi\alpha_n = \frac{2M}{a}. \quad (6.7)$$

The scaling of (6.6) gives

$$\Gamma = \lambda^{-2} \tilde{\Gamma}.$$

Therefore $\Gamma/U_B = O(\lambda^{-2})$ and the upper-layer solution has $u_0 = u_0(R)$, which is consistent with (6.2), and a is a constant, which is consistent with (6.7).

Now the constant a is determined by the initial state of the system (equation (3.3)): either $a = 1$ for a sufficiently shallow chamber or $a = \alpha_c^{-1}$ for a deep chamber.

Therefore, (6.7) represents a straight line in the (Q, M) -plane and its intersection with the curve in figure 5 determines unique values for Q and M , given all the other parameters. For example, if $a = 0.96$ as in the example in §3, figure 5 gives $Q = 20.6$, $M = 9.9$.

The scaling in (6.6) requires that the upper boundary layer is much narrower than the plume. Figure 1 shows photographs of the deep chamber experiments and the cell-rich upper boundary layer does appear to be thinner than the plume so in that respect, at least, the model is in qualitative agreement with the experiments.

7. The two-dimensional problem

The two-dimensional problem is handled in a similar manner to the three-dimensional one. As before, we study the case where $\beta\gamma \gg 1$ and consider three separate regions of fluid.

7.1. Upper boundary layer in two dimensions

In the two-dimensional upper boundary layer we write the governing equations in terms of Cartesian coordinates X and Z and write the velocity as $U = (U, 0, W)$. We rescale the equations using the same scaling as in three dimensions and neglect terms which are obviously $O(\lambda^2)$ compared with the leading ones to obtain

$$\lambda^2 U_B (un_X + wn_z) = n_{zz} - 2 \frac{\partial}{\partial z} (nC_z), \quad (7.1a)$$

$$C_{zz} - n = \frac{\lambda^2 U_B}{\delta} (uC_X + wC_z), \quad (7.1b)$$

$$u_X + w_z = 0, \quad (7.1c)$$

$$Sc^{-1} \lambda^2 U_B (uu_X + wu_z) = u_{zz} - \frac{\lambda^2 P_B}{U_B} p_X, \quad (7.1d)$$

$$Sc^{-1} \lambda^2 U_B (uw_X + ww_z) = w_{zz} + \frac{\Gamma n}{U_B} - \frac{P_B}{U_B} p_z, \quad (7.1e)$$

where the subscripts denote differentiation. The boundary conditions at $z = 0$ are

$$n_z - 2nC_z = 0, \quad C = w = u_z = p_X = 0.$$

We expand n , C and u in powers of λ as in (3.5) for the three-dimensional case and assume that $\lambda^2 U_B \ll 1$ so that advection is unimportant at leading order in (7.1a, b). Leading order in equations (7.1a, b) gives equations (3.6a, b) which have the solution n_0 , θ_0 given in (3.3), where a may be a function of X .

If $U_B \lambda^2 Sc^{-1} \ll 1$, the leading-order terms in equations (7.1d, e) give equations (3.6c, d) with R replaced by X . The solution to these equations is similar to that in the axisymmetric case. If $\Gamma/U_B \gg \lambda^{-2}$, we find that a must be constant. If $\Gamma/U_B = \lambda^{-2}$, we must have $u_0 = u_0(X)$ and a constant and if $1 \ll \Gamma/U_B \ll \lambda^{-2}$, we must also have $u_0 = u_0(X)$ but a may be a function of X .

7.2. Two-dimensional falling plumes

The similarity solution for a three-dimensional axisymmetric descending plume of cell-rich fluid was described in §4. We will now discuss the two-dimensional plume and show that it is not possible to find a similarity solution which satisfies realistic boundary conditions and has non-zero constant cell flux in the plume.

In the plume we scale the horizontal coordinate as $X = \epsilon x$, and N, θ, W, P and U as in (4.1b). The scaling factors N_A, C_A, W_A and P_A , which are chosen so that appropriate terms are retained in the governing equations, have the same values as in three dimensions. Using these scalings and retaining only the leading-order terms in the governing equations gives, after some manipulation,

$$u \frac{\partial n}{\partial x} + w \frac{\partial n}{\partial Z} + 2 \frac{\partial n}{\partial x} \frac{\partial C}{\partial x} + 2n \frac{\partial^2 C}{\partial x^2} - \frac{\partial^2 n}{\partial x^2} = 0, \quad (7.2a)$$

$$\frac{\partial^2 C}{\partial x^2} - \frac{1}{\delta} \left(u \frac{\partial C}{\partial x} + w \frac{\partial C}{\partial Z} \right) - n = 0. \quad (7.2b)$$

$$\frac{\partial u}{\partial x} + \frac{\partial w}{\partial Z} = 0, \quad (7.2c)$$

$$Sc^{-1} \left(u \frac{\partial^2 w}{\partial x^2} + w \frac{\partial^2 w}{\partial x \partial Z} \right) = \tilde{F} \frac{\partial n}{\partial x} + \frac{\partial^3 w}{\partial x^3}. \quad (7.2d)$$

Symmetry about $x = 0$ requires that at $x = 0$

$$\frac{\partial n}{\partial x} = \frac{\partial C}{\partial x} = u = \frac{\partial w}{\partial x} = 0. \quad (7.3a)$$

At the edge of the plume the cell concentration, the oxygen gradient and the vertical fluid velocity should tend to zero. These boundary conditions are as $x \rightarrow \infty$

$$n \rightarrow 0, \quad \frac{\partial C}{\partial x} \rightarrow 0, \quad w \rightarrow 0. \quad (7.3b)$$

We now seek a similarity solution to equations (7.2a–d) of the form given in (4.4). Substituting this solution into equations (7.2a, b, d) and equating powers of Z in each term gives $a = \frac{1}{2}$, $b = 0$, $c = -1$, $d = 0$, which is identical to the three-dimensional case. We therefore define the similarity variable $\eta = x/Z^{1/2}$ and pose a solution:

$$n = Z^{-1}H(\eta), \quad C = G(\eta), \quad \psi = Z^{1/2}F(\eta), \quad u = \frac{1}{2}Z^{-1/2}(F - \eta F'), \quad w = -F',$$

where primes denote differentiation with respect to η . Substituting this solution into equations (7.2a–d) gives

$$\frac{1}{2}H'F + F'H + \gamma H'G' + \gamma HG'' - H'' = 0, \quad (7.4a)$$

$$G'' - \frac{1}{2\delta}G'F - H = 0, \quad (7.4b)$$

$$F^{IV} - \frac{1}{2}Sc^{-1}(FF''' + F'F'') - \tilde{F}H' = 0. \quad (7.4c)$$

The boundary conditions become at $\eta = 0$

$$H' = G' = F = F'' = 0,$$

as $\eta \rightarrow \infty$

$$H \rightarrow 0, \quad G' \rightarrow 0, \quad F' \rightarrow 0.$$

Integrating equation (7.4a) once with respect to η and applying the boundary conditions at $\eta = 0$ gives

$$\frac{1}{2}HF + \gamma HG' - H' + \frac{1}{2} \int_0^\eta HF' d\eta = 0; \quad (7.4d)$$

the presence of the last term distinguishes this equation from the corresponding equation in the axisymmetric case (4.7a). Applying the boundary condition $H \rightarrow 0$ as $\eta \rightarrow \infty$ (which means that $H' \rightarrow 0$ as $\eta \rightarrow \infty$) gives

$$\int_0^\infty HF' d\eta = -Q = 0, \tag{7.5}$$

where Q is defined in (4.9). The cell flux in the plume is $\int_0^\infty nw dx = QZ^{-1/2}$, which is zero from (7.5). This is clearly not the case in any plume driven by the negative buoyancy of the cells, such as those in the experiments of figure 1. Going to higher order in Z^{-1} does not improve matters.

If Q was non-zero the cell flux in the plume would not be constant. This is not realistic since it would involve cells swimming into or out of the plume and the cell concentration at the edge of the plume would be non-zero, indicating that the cell concentrations in the plume and outer region are of similar magnitude. This is inconsistent with a boundary-layer scaling and is not borne out by the experiments of figure 1. We therefore conclude that although equations (7.2a–d) may have a solution which satisfies the boundary conditions (7.3a, b) and gives non-zero cell flux in the plume, such a solution will not be a similarity solution of the form (4.4).

The difference between the two-dimensional problem of Yih (1952) for a thermal plume and this bioconvection plume lies in the interaction between the cells and the oxygen. If chemotaxis or oxygen consumption are not important in the plume ($\gamma = 0$ or $\beta = 0$ in 7.2a–d) it is possible to find a similarity solution which satisfies the boundary conditions (7.3a, b) and has non-zero constant cell flux in the plume; in fact, this is simply the solution of Yih (1952) with the plume width h proportional to $Z^{2/5}$ and the similarity variable $\eta = x/Z^{2/5}$. In the three-dimensional axisymmetric plume the chemotaxis and oxygen consumption terms do not affect the similarity solution, but in the two-dimensional case they do.

7.3. Two-dimensional outer flow

In two dimensions, the governing equations in the outer region are the continuity equation and (5.1), as in three dimensions. We write U in terms of a stream function, ψ , and solve (5.1) in the region $0 < Z < 1$ and $0 < X < d$. As in the three-dimensional case, we impose stress-free boundary conditions at the upper and lower surfaces: at $Z = 0, 1$

$$\frac{\partial\psi}{\partial X} = \frac{\partial^2\psi}{\partial Z^2} = 0. \tag{7.6a}$$

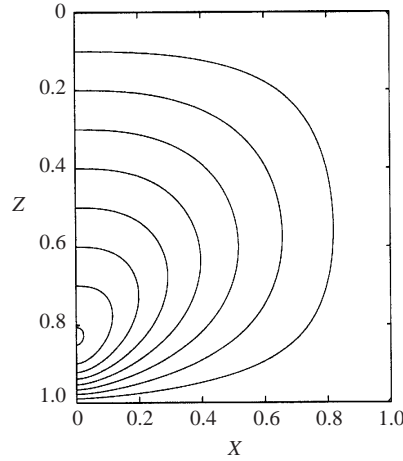
At the outer boundary $X = d$, we impose

$$\frac{\partial\psi}{\partial Z} = 0, \quad \frac{\partial^2\psi}{\partial X^2} = 0. \tag{7.6b}$$

The boundary conditions at the edge of the plume ($X = 0$) are set by the solution in the plume. In two dimensions, there is no similarity solution so we arbitrarily impose boundary conditions similar to those in three dimensions. We will require that $w \rightarrow 0$ and $u \rightarrow -M$ at the edge of the plume, where w and u are the scaled variables in the plume. These boundary conditions are therefore at $X = 0$

$$\frac{\partial\psi}{\partial X} = 0, \quad \frac{\partial\psi}{\partial Z} = \epsilon^{-1}\tilde{\alpha}, \tag{7.6c}$$

where $\tilde{\alpha}$ is given in (5.3). The ϵ^{-1} factor arises because in two dimensions the horizontal fluid velocity in the plume, u , is $O(\epsilon^{-1})$.

FIGURE 10. Streamlines for the two-dimensional outer flow when $M = 1$, $d = 1$.

Proceeding as in three dimensions, we find that the general solution for the outer flow which satisfies the boundary conditions (7.6a) is

$$\psi = \sum_n \sin(n\pi Z)(\tilde{A}_n e^{n\pi X} + \tilde{B}_n X e^{n\pi X} + \tilde{C}_n e^{-n\pi X} + \tilde{D}_n X e^{-n\pi X}).$$

The coefficients \tilde{A} , \tilde{B} , \tilde{C} and \tilde{D} are chosen so that the boundary conditions at $X = 0, d$ are satisfied and are:

$$\tilde{A}_n = (1 + e^{2n\pi d} + 2n\pi d e^{2n\pi d})q_n, \quad (7.7a)$$

$$\tilde{B}_n = (-n\pi - n\pi e^{2n\pi d})q_n, \quad (7.7b)$$

$$\tilde{C}_n = (-e^{2n\pi d} + 2n\pi d e^{2n\pi d} - e^{4n\pi d})q_n, \quad (7.7c)$$

$$\tilde{D}_n = (-n\pi e^{2n\pi d} - n\pi e^{4n\pi d})q_n, \quad (7.7d)$$

where

$$q_n = \epsilon^{-1} \alpha_n (1 + 4n\pi d e^{2n\pi d} - e^{4n\pi d})^{-1}.$$

In figure 10, we plot the streamlines using the first forty terms of the series for $d = 1$ and $M = 1$. The choice of the value of M is arbitrary since we have no plume solution to which we can match it.

We now attempt to match the solutions in the three different regions in the same way as for the three-dimensional axisymmetric case. The horizontal fluid velocity at the edge of the upper boundary layer $Z = \lambda$ in the outer region is

$$U = \sum_n n\pi(\tilde{A}_n e^{n\pi X} + \tilde{B}_n X e^{n\pi X} + \tilde{C}_n e^{-n\pi X} + \tilde{D}_n X e^{-n\pi X}) + O(\lambda^2), \quad (7.8)$$

which is $O(\epsilon^{-1})$, indicating that in two dimensions $U_B = O(\epsilon^{-1})$. We write $u_{0\epsilon} = u_0(X = \epsilon)$ for the fluid velocity in the upper layer at the edge of the plume $R = \epsilon$ and equation (7.8) gives

$$U_B u_{0\epsilon} = \epsilon^{-1} \sum_n n\pi \alpha_n.$$

Using this we find that the fluid flow out of the upper boundary layer into the plume

is $O(\lambda U_B u_{0\epsilon}) = O(\lambda \epsilon^{-1})$ and the cell flux out of the upper boundary layer into the plume is $O(\lambda U_B u_{0\epsilon} \lambda^{-1}) = O(\epsilon^{-1})$.

We have no two-dimensional similarity solution in the plume, but we assume that the solution is like the three-dimensional solution in that the cell flux in the plume is constant and the fluid flux is proportional to Z . Then the cell flux in the plume is $O(\lambda \epsilon^{-3})$ and the fluid flux is $O(\lambda \epsilon^{-1})$. As in the three-dimensional case, it follows that the fluid flux in the upper boundary layer agrees with that in the plume, and the cell flux in the upper boundary layer agrees with that in the plume if $\epsilon = \lambda^{1/2}$. However, this is not a firm conclusion since it is based on an assumption about the solution in the plume. Thus, the two-dimensional case remains unresolved.

8. Conclusion

In this paper we have endeavoured to model deep chamber bioconvection experiments as shown in figure 1. We considered three different regions: a thin upper boundary layer of thickness λ , a falling plume of width ϵ and the region outside the plume. We considered only the upper part of the chamber, in which $\theta > 0$ and the bacteria are active. We examined the two-dimensional and the three-dimensional axisymmetric cases.

Hillesdon *et al.* (1995) showed that the steady-state, non-convective solution has a thin upper boundary layer in the limit $\beta\gamma \gg 1$. This boundary layer has thickness $\lambda = 2/\beta\gamma$ and we used the scaling of Hillesdon *et al.* (1995) to find solutions in the upper boundary layer. The solution is essentially the same in two and three dimensions and depends on the magnitude of the Rayleigh number, Γ , and the scaling of the horizontal fluid velocity in the upper layer, U_B .

The upper layer is unstable and this instability takes the form of falling plumes of cell-rich fluid. In three dimensions, we found a similarity solution for the plume, similar to that for thermal convection, in which the width of the plume is proportional to $\lambda^{1/2} Z^{1/2}$ and the cell flux in the plume is constant. At the edge of the plume $ru \rightarrow -M$ indicating that the plume entrains fluid from the outer region. In two dimensions, it is not possible to find a similarity solution for the plume which takes account of all the terms, has non-zero cell flux and satisfies the boundary conditions, because of the interaction of the n and θ terms.

The falling plume entrains fluid and drives a flow in the outer, cell-depleted region. In three dimensions, the outer flow can be found as a Fourier–Bessel series and we can use this solution to predict the horizontal fluid velocity in the upper boundary layer. We can find a similar solution for the outer flow in two dimensions, if we assume certain boundary conditions at the edge of the plume. Finally, we matched the solutions at the boundaries of the different regions and found that the solutions are consistent if the width of the plume, ϵ , is $\lambda^{1/2}$ (6.6).

According to the three-dimensional similarity solution, the width of the plume is proportional to $\lambda^{1/2} Z^{1/2}$ so that the width of the plume increases as Z increases. At sufficiently large Z , ($Z = O(\lambda^{-1/2})$), the assumption that the plume is narrow will no longer hold, the $\partial/\partial Z$ terms neglected in (4.3a–c) will become important and the similarity solution will break down. The plume solution described here assumes that $\theta > 0$ so that all the bacteria are actively swimming. When the plume reaches the lower, oxygen-depleted region ($Z = 1$) the solution described here will no longer be valid. Since $\lambda \ll 1$, the plume will reach the lower region before the similarity solution breaks down.

The model for the falling plume experiments described in this chapter is only quasi-steady. The cell-rich upper boundary layer feeds a plume which takes bacteria

from the upper boundary layer to the lower part of the fluid. We have assumed that once the bacteria reach the lower part of the fluid (where $\theta = 0$) they remain there. We have also assumed that the cell concentration in the outer region is negligible and that there is no significant bacterial upswimming from the outer region to the upper boundary layer. The upper boundary layer is losing cells to the plume without gaining any from the outer region and the concentration of bacteria in the upper layer is therefore decreasing. This means that a and hence Q will vary slowly with time, which could be an interesting development for future study. At some time the cell concentration will become less than $O(\lambda^{-1})$ and the solution described here will break down.

In the experiments of figure 1, the plume carries oxygen into the lower part of the fluid, thereby resuscitating cells which had become inactive because of a lack of oxygen. The model described here does not take this effect into account and is valid only at times before it becomes important. It is likely that a numerical simulation would be required to capture the full behaviour of the system.

We would like to thank the EPSRC for the award of a Research Studentship to A. M. M. and a Senior Fellowship to T. J. P. The NRK routine was kindly provided by Dr D. R. Moore. We are also grateful to Professor J. O. Kessler for permission to re-use figure 1, and to him, Dr N. A. Hill, Dr S. Ghoraï and Dr M. R. E. Proctor for many helpful discussions.

REFERENCES

- BEARON, R. N. & PEDLEY, T. J. 2000 Modelling run-and-tumble chemotaxis in a shear flow. *Bull. Math. Biol.* **62**, 775–791.
- BEES, M. A. & HILL, N. A. 1998 Linear bioconvection in a suspension of randomly swimming, gyrotactic micro-organisms. *Phys. Fluids* **10**, 1864–1891.
- CASH, J. R. & MOORE, D. R. 1980 A high order method for the numerical solution of two-point boundary value problems. *BIT* **20**, 44–52.
- GHORAÏ, S. & HILL, N. A. 1999 Development and stability of gyrotactic plumes in bioconvection. *J. Fluid Mech.* **400**, 1–31.
- HILL, N. A., PEDLEY, T. J. & KESSLER, J. O. 1989 Growth of bioconvection patterns in a suspension of gyrotactic microorganisms in a layer of finite depth. *J. Fluid Mech.* **208**, 509–543.
- HILLEDON, A. J. 1994 Pattern formation in a suspension of swimming bacteria. PhD thesis, University of Leeds.
- HILLEDON, A. J. & PEDLEY, T. J. 1996 Bioconvection in suspensions of oxytactic bacteria: linear theory. *J. Fluid Mech.* **324**, 223–259.
- HILLEDON, A. J., PEDLEY, T. J. & KESSLER, J. O. 1995 The development of concentration gradients in a suspension of chemotactic bacteria. *Bull. Math. Biol.* **57**, 299–344.
- KELLER, E. F. & SEGEL, L. A. 1971a Model for chemotaxis. *J. Theor. Biol.* **30**, 225–234.
- KELLER, E. F. & SEGEL, L. A. 1971b Travelling bands of chemotactic bacteria. *J. Theor. Biol.* **30**, 235–248.
- KESSLER, J. O. 1985 Hydrodynamic focusing of motile algal cells. *Nature* **313**, 218–220.
- KESSLER, J. O., HOELZER, M. A., PEDLEY, T. J. & HILL, N. A. 1994 Functional patterns of swimming bacteria. In *Mechanics and Physiology of Animal Swimming* (ed. L. Maddock, Q. Bone & J. M. V. Rayner), pp. 3–12. Cambridge University Press.
- KUIKEN, H. K. & ROTEM, Z. 1971 Asymptotic solution for plume at very large and small Prandtl numbers. *J. Fluid Mech.* **45**, 585–600.
- LYNE, W. H. 1971 Unsteady viscous flow in a curved pipe. *J. Fluid Mech.* **45**, 13–31.
- METCALFE, A. M. 1998 Nonlinear aspects of bioconvection in suspensions of swimming bacteria. PhD thesis, University of Leeds.
- METCALFE, A. M. & PEDLEY, T. J. 1998 Bacterial bioconvection: weakly nonlinear theory for pattern selection. *J. Fluid Mech.* **370**, 249–270.

- PEDLEY, T. J. & KESSLER, J. O. 1990 A new continuum model for suspensions of gyrotactic microorganisms. *J. Fluid Mech.* **212**, 155–182.
- PLATT, J. R. 1961 'Bioconvection patterns' in cultures of free-swimming organisms. *Science* **133**, 1766–1767.
- ROBERTS, G. O. 1977 Fast viscous convection. *Geophys. Astrophys. Fluid Dyn.* **8**, 197–233.
- WORSTER, M. G. 1986 The axisymmetric laminar plume—asymptotic solution for large Prandtl number. *Stud. Appl. Math.* **75**, 139–152.
- YIH, C.-S. 1951 Free convection due to a point source of heat. In *Proc. 1st US Nat. Cong. Appl. Mech.* (ed. E. Sternberg), pp. 941–947.
- YIH, C.-S. 1952 Laminar free convection due to a line source of heat. *Trans. Am. Geophys. Union* **33**, 669–472.